PAPER • **OPEN ACCESS**

Increase of the photoconductivity quantum yield in silicon irradiated by neutrons to extremely high fluences

To cite this article: Juozas V Vaitkus *et al* 2022 *J. Phys. D: Appl. Phys.* **55** 395104

OPEN ACCESS
IOP Publishing
Journal of Physics D: Applied Physics
J. Phys. D: Appl. Phys. **55** (2022) 395104 (8pp)
https://doi.org/10.1088/1361-6463/ac7f65

Increase of the photoconductivity quantum yield in silicon irradiated by neutrons to extremely high fluences

Juozas V Vaitkus[1,*], Michael Moll[2], Vaidotas Kažukauskas[1] and Vilius Vertelis[1]

[1] Institute of Photonics and Nanotechnology, Faculty of Physics, Vilnius University, Saulėtekio al. 3, Vilnius LT-10222, Lithuania
[2] CERN, CH-1211 Geneva 23, Switzerland

E-mail: juozas.vaitkus@ff.vu.lt

Received 8 March 2022, revised 22 June 2022
Accepted for publication 7 July 2022
Published 21 July 2022

Abstract

An enhanced quantum yield observed in silicon ionizing radiation detectors, neutron-irradiated to extremely high fluences, could be attributed to impact ionization via deep levels. The quantum yield was investigated by the intrinsic photoconductivity optical spectroscopy in silicon irradiated by neutrons to a wide range of fluences up to 1×10^{17} neutron cm^{-2}. An increase of quantum yield was observed in highly irradiated samples. We have demonstrated that the quantum yield enhancement could be attributed to the impact ionization via deep levels, this process being presumably related to disordered defect clusters regions in Si. The proposed mechanism explains the observed decrease of the impact ionization energy by at least an order of magnitude at low temperature. The impact ionization energy values of up to 0.30–0.36 eV and less, and 0.38–0.40 eV were determined at $T \sim 21$–33 K and at $T = 195$ K, respectively.

Keywords: photoconductivity, quantum yield, silicon, impact ionization, defect cluster

(Some figures may appear in colour only in the online journal)

1. Introduction

Silicon particle detectors, which play the central role in high energy physics research, suffer from a reduction of efficiency due to radiation damage. The challenge of retaining the required efficiency in these detectors with increasing irradiation fluences can be addressed either by increasing the bias voltage following irradiation [1] or by sophisticated detector designs, as e.g. demonstrated for the Low Gain Avalanche Diode (LGAD) technology [2, 3], in which an implanted ion layer is used to create the effective multiplication of non-equilibrium carriers by impact ionization.

An influence of the radiation-induced damage on the electron impact ionization coefficient has been observed in [4, 5]. A small but distinct reduction of its value at high fluence (in the range of 10^{14}–10^{15} neutrons cm^{-2}) with respect to the unirradiated silicon samples was reported in [4]. The charge multiplication effect has been also observed in Si strip detectors irradiated by up to 10^{16} neutrons cm^{-2} in experiments employing laser generated non-equilibrium charge carriers [5]. These results provide a strong motivation to investigate the photogeneration quantum yield in Si samples irradiated by similar neutron fluence striving to determine the energy necessary for carrier impact ionization.

Photoconductivity depends on the absorption of incident photons, generation of electron–hole pairs, and carrier transport mechanisms (diffusion and drift) [6]. To cause excitation,

* Author to whom any correspondence should be addressed.

the incident photon energy must exceed the semiconductor bandgap (so called intrinsic excitation), or excite charge carriers from impurity energy levels within the bandgap (extrinsic excitation). The electrical conductivity increase depends on the number of the photogenerated electron–hole pairs, depending also on the quantum yield, as well as on carrier mobility and lifetime. All these factors are also affected by the recombination centers in the bulk and at the surface of the crystal.

This paper presents an analysis of the photoconductivity spectral dependencies in Si radiation detectors, irradiated by neutrons to very high fluences (10^{15}–10^{17} n cm^{-2}). The main attention is being paid to the intrinsic photoconductivity region. We report a significant increase of the quantum yield in the samples irradiated to the highest neutron fluences, which could be attributed to the impact ionization via the defect states created by irradiation.

2. Methods and samples

We were focusing on the intrinsic photoconductivity region, in which the excess carriers are generated by the above-band-gap photons. In this region the photocurrent spectral dependence can be approximated by an expression valid for thick samples with a thickness d which significantly exceeds the diffusion length L of the carriers ($d \gg L$) [6]:

$$I\text{photo} = \frac{eqwLJ\tau\mu\,(1-R)\,E}{L+s\tau} \times \left(1+\frac{s\tau}{L\,(1+\alpha L)}\right), \quad (1)$$

here e—electron charge, q—quantum yield, w—sample width, J—density of photons cm^{-2}, τ—electron lifetime, μ—electron mobility, R—reflection coefficient, E—electric field created by bias voltage V, s—surface recombination rate, α—light absorption coefficient. The diffusion length depends on electron lifetime and mobility according to the well known relation:

$$L = \sqrt{D\tau} = \sqrt{\left(\mu\frac{kT\tau}{e}\right)}, \quad (2)$$

where k—Boltzmann constant, T—temperature, e—electron charge.

We have investigated Si samples fabricated by the magnetic Czochralski (MCZ) method. Measurements were performed on two types of samples: strip sensors (0.3 mm thick, with 8 mm gap between 6 mm wide contacts), and microstrip sensors (0.3 mm thick, 10 microstrips on each sample, 43 μm between strips) (figure 1).

The strip samples have been produced by Hamamatsu company in Japan by the CERN RD50 project WODEAN. The microstrip samples was of type 'RD50-20 n-type MCZ'. They have been produced by CNM, Barcelona, Spain in 2006 on 4 inch n-type MCZ wafers produced by Okmetic, Finland. The measurements have been performed between the neighboring microstrips.

The samples were irradiated in the Ljubljana University TRIGA reactor by reactor neutrons with fluences ranging from 10^{13} up to 10^{17} n cm^{-2} (1 MeV neutron equivalent fluence). The time elapsed between the irradiation and begin of the experiments was usually one week. However, during the samples they were kept for two days in a 'cold box' which temperature at delivery was −10 °C and we want to stress that all the time when the samples were not investigated they were stored in a freezer at about −20 °C in order to prevent the thermal annealing of the created defects. The displacement damage is originating from the fast neutrons which have a NIEL which is several orders of magnitude higher than the thermal neutrons. The sample surfaces were passivated by a SiO_2 layer, which thickness was 800–1000 nm.

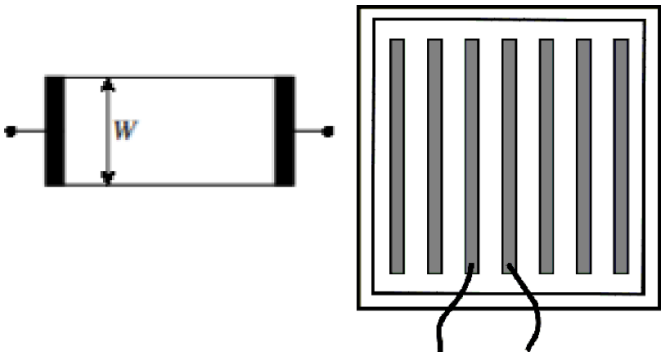

Figure 1. The sketch of investigated samples. At left the strip sample, at right the microstrip sample.

The samples were placed in a closed-cycle Helium cryostat (ARSCryo), with the temperature being controlled by the Scientific Instruments 9700. The current was measured by an HP4140B electrometer. The samples were optically excited using a DMR4 double prism monochromator. The measurements were performed keeping the same photon density of 7.8×10^{13} photons cm^{-2} s^{-1} at all photon energies. The data were processed by a PC with a general purpose interface bus interface.

The I–V characteristics of the samples were nearly linear. The presented results were obtained at an electric field strength of 63 V cm^{-1} in the strip samples and 23 V cm^{-1} (between the strips) in the microstrip samples. The measurements of photocurrent were usually performed first by increasing the energy of photons and afterwards by decreasing it to avoid pre-excitation of the samples. In each direction about 1500 readings were taken and the time of the scans in one direction was about 15–20 min. After the measurement upon increasing the quanta energy, the samples were left to relax for about ∼5 min under the same excitation, then the measurements in an opposite direction were started. The differences in these results show the role of non-equilibrium carrier-induced persistent current, which was observed in the extrinsic region.

An example of this dependence is presented in figure 2.

The data evidence that the differences in the photocurrent taken by increasing photon energy and that measured by decreasing photon energy disappear above the photon energy of approximately 0.97 eV. It proves that in the spectral region of interest, i.e. in the intrinsic photoconductivity region, measurements of the spectra in both directions, i.e. by increasing

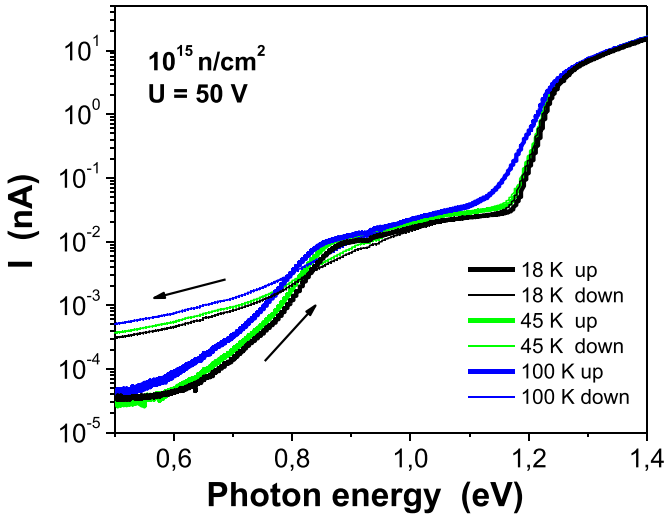

Figure 2. Photocurrent spectral dependencies of the sample irradiated by 10^{15} n cm^{-2}. The measurements of the photocurrent were performed first by increasing the energy of photons and afterwards by decreasing it. Measurement temperatures and other details are indicated in the legend. Arrows indicate the scanning directions.

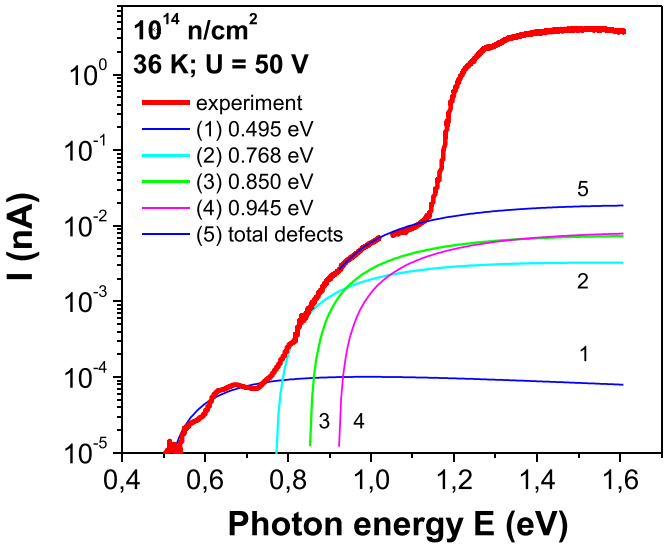

Figure 3. Spectral dependencies of the photocurrent in the strip sample irradiated by neutrons to a fluence of 1×10^{14} n cm^{-2} measured at 36 K temperature. Red thick line—experiment, other numbered lines—modelled influence of the deep levels according to equation (3).

and decreasing photon energies, are not relevant. Thus, the spectra presented and discussed below were all measured by increasing photon energy.

3. Results

According to equation (1) the quantum yield dependence on photon energy is a main factor defining the photocurrent spectral dependence in the samples with passivated surface (i.e. $s = 0$), if all photons have been absorbed in the sample. At measurement temperatures this was the case for photons having the energy above 1.42 eV [7] (i.e. $d \times \alpha \sim 0.01$).

The spectral dependence of photo response displayed a classical behavior in the sensors irradiated to a relatively low neutron fluence (10^{14} n cm^{-2}) as shown in figure 2. The contribution of deep levels was observed upon below band-gap illumination. In the intrinsic excitation region, the photo response increased up to the point where, due to the increasing light absorption coefficient and the influence of surface recombination, it started to decrease slightly, as shown in figure 3. Such behavior was also observed in previous experiments performed after neutron irradiation, see e.g. [8], paid to the intrinsic photoconductivity region. Figure 3 also demonstrates the results of analyses using the method of determination of the deep level optical activation energies, as described in [8]. It proves that the deep defect states are prominent in the irradiated samples, and these states could be effective in the impact ionization processes as described below.

The photoconductivity spectra were analyzed using the deep center model with δ-potential (Lukovsky model) [9]. The cross-section of photo-ionization was simulated by the formula

$$I \sim m \times \Delta E_M{}^{0.5}(h\nu - \Delta E_M)^{1.5}/h\nu^3, \qquad (3)$$

where ΔE_M is the optical activation energy of the deep center, $h\nu$ is the photon energy and m is the concentration of filled deep center. The presented contribution of the deep levels to the photocurrent was evaluated by subtracting the inputs of the shallower levels.

Figure 3 clearly demonstrates that the photoconductivity spectra follow the dependencies described by equation (1) with quantum yield being equal to 1. Characteristically, no photoconductivity increase was observed in the samples irradiated by less than 1×10^{15} n cm^{-2} fluence in the spectral region beyond $h\nu > 1.4$ eV. The same behavior has been observed in [8, 10].

However, significant changes of the spectral dependencies were observed in the samples irradiated by 1×10^{15} n cm^{-2} and beyond (figure 4). Instead of the saturation of photo response or its decrease due to the surface recombination at the photon energy at which all photons are absorbed, i.e. at photon energies above about 1.4 eV in figure 3, an increasing photo response with increasing photon energy was observed above the band gap of Si as shown in figure 4. For the sake of clarity, the data are presented in both linear and logarithmic scaling. Following equation (1), the growth of the photocurrent with increasing photon energy in the high absorption region of the spectrum could be explained by an increase of the quantum yield. Such a dependence is clearly seen in the samples irradiated up to 1×10^{15} and 3×10^{16} n cm^{-2}. In the other samples this process starts at even lower photon energies. At the experiment temperature the bandgap of Si is 1.19 eV [11], thus at lower photon energies the extrinsic photocurrent can be caused only by excitation from deep states in the band gap. A comparison of extrinsic photocurrents in, e.g. [8, 10], had proved their dependences on the deep level densities in the samples irradiated to various neutron fluences. The intrinsic photocurrent, according to equation (1), should also be dependent on

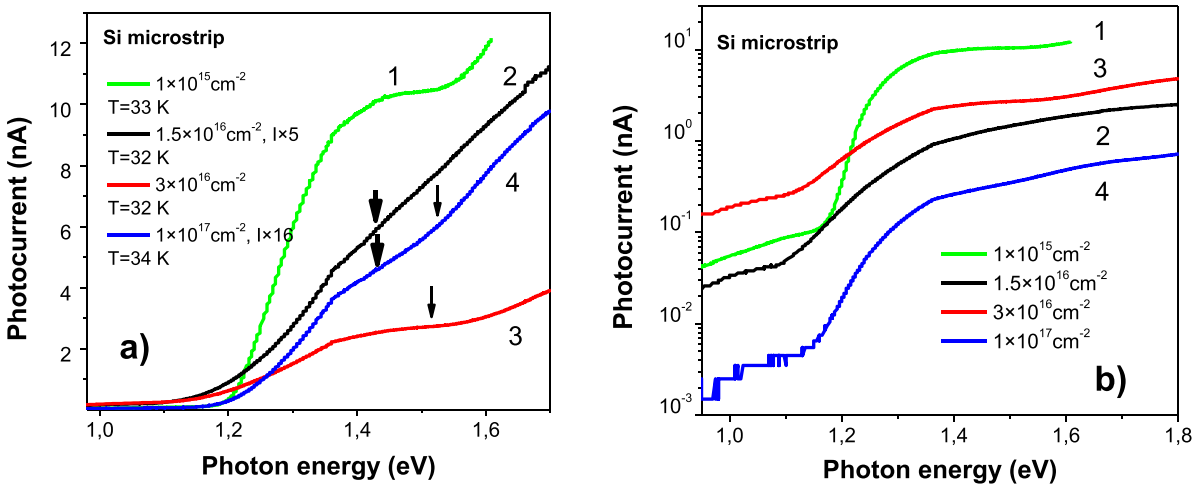

Figure 4. Spectral dependencies of the photocurrent in the microstrip samples irradiated by different neutron fluences as indicated on figures: 1–1 × 10^{15} n cm^{-2}; 2–1.5 × 10^{16} n cm^{-2}; 3–3 × 10^{16} n cm^{-2} and 4–1 × 10^{17} n cm^{-2}. (a)—linear scale, (b)—logarithmic scale. Measurement temperatures are given in the legend. Note that on the left figure 3(a) black and blue data are multiplied by factors of 5 and 16 respectively for the sake of clarity. The thin arrows show the approximate photon energies at which the quantum yield increase starts, and the thick arrows mark the photon energy beyond which all photons are absorbed in the sample.

Table 1. Thresholds of the quantum yield increase and minimal electron impact ionization energies evaluated in different samples and measurement temperatures. The bandgap of Si was obtained by the well-known approximation: $Eg = 1.166 - 4.73 \times 10^{-4} \times T^2/(T+636)$ [10].

Fluence (n cm^{-2})	T, K	Threshold (eV)	Bandgap (eV)	Minimal electron impact ionization energy (eV)
1 × 10^{15}	33	1.497–1.509	1.165	0.34
	120	1.524–1.528	1.157	0.37
	195	1.524–1.532	1.144	0.38
1 × 10^{16}	21	1.461–1.466	1.1657	0.30
	120	1.524–1.541	1.157	0.38
	195	1.541–1.549	1.144	0.40
1.5 × 10^{16}	32	1.42–1.44	1.165	>0.26
3 × 10^{16}	21	1.519–1.524	1.1657	0.36
	32	1.511–1.528	1.165	0.36
	50	1.537	1.164	0.37
	100	1.554	1.160	0.39
1 × 10^{17}	34	>1.42, 1.524	1.165	>0.26, 0.36

the lifetime and mobility of the charge carriers; however, they do not contribute to the spectral dependencies in the samples with passivated surfaces.

It is seen in figure 4 that the quantum yield starts to grow well above the bandgap as indicated by the thin arrows in the samples irradiated to 1 × 10^{15} and 3 × 10^{16} n cm^{-2}. This is well pronounced but in the other samples the quantum yield increase start was difficult to establish as it started at lower photon energies at which all photons have been absorbed. At this region it is a superposition of the intrinsic and extrinsic mechanisms of the photocurrent, that did not permit to evaluate the photon energy at which quantum yield increase started. In such cases, in table 1, which presents all results, values were given for photon energies at which all photons have been absorbed (the thick arrows in figure 4), marking that the true values could be lower. A more complicated case was encountered in the sample irradiated by 1 × 10^{17} n cm^{-2}, which had two regions where the quantum yield increases: the quantum yield increase started at photon energy less than 1.42 eV (the thick arrow at figure 4), and the additional quantum yield increase beginning could be set at photon energy approximately equal to 1.52 eV.

The quantum yield increase can happen if an electron, generated in the conduction band and having the excess energy, would relax to an energetically lower state in the conduction band exciting another electron from the defect state into the conduction band. Such impact ionization would lead to an increase in the carrier density (carrier multiplication), inducing in this way a sharper growth of the photocurrent. Following the model presented in the discussion below, deep levels had to participate in this process. The energies of the levels, that could participate in the impact ionization, were obtained by subtracting of the Si bandgap width from the average value of photon energies at which the thresholds of the quantum yield

increase were identified. The thresholds of the quantum yield increase and the energies of the levels that were taking part in the impact ionization are presented in table 1.

4. Discussion

The increase of the photo-response at photon energies above the bandgap of Si can occur only due to an increase of the quantum yield. Previous publications have demonstrated an increase of the quantum yield upon excitation by photons with energy above approximately 3.2 eV [12–14], and a reasonable agreement between the experimental values and the theoretical spectral dependence has been obtained [15]. The energy of the electron–hole pairs creation equal to 3.6 ± 0.3 eV [16] was also established, and this value corresponded to the value obtained theoretically [17]. In this and other analysis of this phenomenon [15, 17, 18] an electron, which has excess energy, relaxes to an energetically lower state inducing excitation of a valence band electron into the conduction band. This impact ionization causes an increase of the carrier density (carrier multiplication). The same mechanism is valid also for holes. In semiconductor structures, these relaxation channels follow the restrictions imposed by energy and momentum conservation, therefore energy exceeding the bandgap is necessary, due to the bandgap energy dispersion.

In our study the threshold of the quantum yield increase as function of photon energy occurred at a much lower energy than observed in earlier works [12–14]; therefore, a new model of impact multiplication of free electrons is proposed.

The mechanism of the impact ionization should be considered as the inverse of the Auger recombination [18, 19]. In this process, a high energy electron impacts an electron on an impurity level and loses its energy exciting the latter. As a consequence, both electrons will eventually be found close to the minimum of the conduction band. Logically, only electrons with energy exceeding the energy of the impurity ground state may take part in the ionization process [19].

Therefore, impact ionization could occur at lower energies than in the intrinsic case, and the minimal electron impact ionization energy corresponds to the activation energy of the deep level involved. As the process in which the deep local levels participate has no restrictions imposed by momentum conservation, a lot of impact trajectories are possible. Figure 5 shows one of them.

Clearly, this kind of impact ionization depends on the concentration of filled levels and the energy levels of states taking part in this process, and so it can be different in different samples. Thus, experimentally it appeared to be a problem to find the states participating in the process. E.g. an analysis of the deep level spectra in similar Si samples irradiated beyond 10^{15} n cm^{-2} [11] did not reveal any filled levels in the bandgap that could take part in the impact ionization process. Our task was, therefore, to identify the states participating in the impact ionization process.

As the increase of the quantum yield was most prominent in Si irradiated to very high neutron fluences, the conclusion

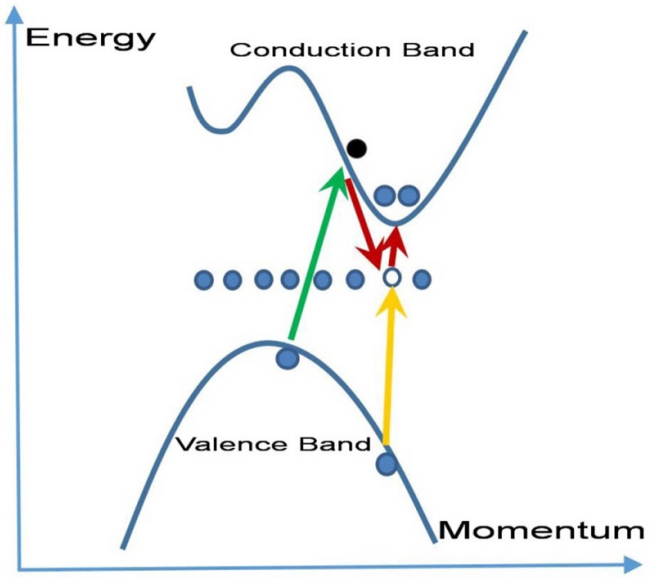

Figure 5. Possible transitions to achieve impact ionization via deep defect levels induced by neutron irradiation. Step 1: photon excites an electron (green line); step 2: electron (black dot) impacts an electron at a local level and excites it into the conduction band, landing itself also in the conduction band minimum (red arrows); step 3: photon-excited electron (yellow line) restores the occupancy of the local level.

might be drawn that disordered regions in Si crystals inevitably take part in the impact ionization. An investigation of carrier mobility in Si irradiated above 10^{16} cm^{-2} fluence identified peculiarities related to the material disorder [20].

High energy hadron interactions with the Si lattice are known to result in the transfer of hadron momentum to the Si lattice atoms creating, due to multiple collisions, a characteristic tree-like structure with several sub-clusters [21]. It has also been shown that neutrons tend to produce isolated dense vacancy clusters with a much lower number of point defects [21]. The electron states in the extended defect regions have been studied by means of computer simulations [22, 23]. It was shown that vacancy clusters in disordered Si create deep energy levels within the bandgap [22–24]. Deep multilevel electron states localized within amorphous disordered regions both with and without vacancies were predicted by density functional theory (DFT) simulations [24].

Clusters of various sizes could be created by a high energy particle (HEP) after collision. To be sure that the small clusters also create deep states in the band-gap, the simulation of the small (∼1 nm size) cluster was performed [25] and is presented in the annex. The results confirm existence of the defect levels in the bandgap of Si in such small clusters.

Thus, the results confirmed existence of the defect levels in the bandgap of Si for many cluster types and, based on results presented in [22–27], the proposed model explains the observed quantum yield enhancement caused by the non-equilibrium carriers. The increase with temperature of the minimal electron impact ionization energies (table 1 and figure 6)

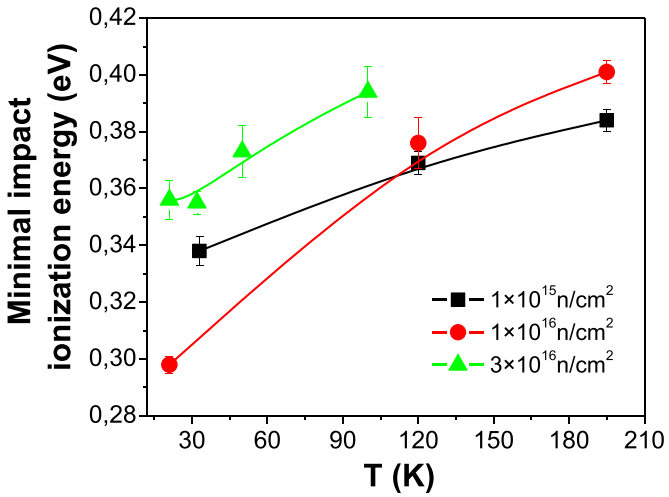

Figure 6. Dependence of the minimal electron impact ionization energy on temperature.

is consistent with the model. At higher temperatures more shallow levels can be emptied and the minimal electron impact ionization energy would increase.

The lack of a direct dependence of minimal electron impact ionization energies on the neutron fluence (table 1) and the quantum yield dependence on the photon energy in samples irradiated to different neutron fluences (figure 3) may be related to the stochastic nature of cluster creation and size distribution. It is clear that the density of defect states in disordered regions is high in the highly irradiated samples, thus they should contribute to the observed effects. Potentially the high efficiency of carrier multiplication in the LGAD detector that exploit deep implants [28] could be influenced by defects related to the disordered layer caused by the ion implantation. Creation of deep levels during the ion implantation was observed in [29]. A possible influence of the impact ionization has also been observed in disordered materials [30].

5. Conclusions

- An enhancement of quantum yield was observed in Si irradiated by neutrons to fluences of 1×10^{15} n cm^{-2} and above upon intrinsic light excitation.
- This effect could be attributed to the impact ionization via deep levels, presumably related to the defect clusters in the disordered regions of the irradiated Si samples.
- A decrease of the energy required for impact ionization (by more than an order of magnitude) should increase the efficiency of detectors irradiated by high fluences. LGAD detectors with their deep implants probably do exploit this effect but do not explicitly take it into account [28, 31].

Data availability statement

The data that support the findings of this study are available upon reasonable request from the authors.

Acknowledgments

This work was performed in the framework of the CERN RD50 collaboration. It was funded by the Lithuanian Academy of Sciences, Grant No. CERN-VU-2019-2022. The authors wish to thank the Transnational Access activity of the European Union's Horizon 2020 Research and Innovation programme, under Grant Agreement No. 654168, for funding the Si samples irradiation. Also authors express gratitude to E Žąsinas for contribution in editing the annex.

Co-authors V K and V V conducted the experiments, co-author M M conducted the editing of data to present and co-author J V V conceptualized the work.

Annex

The results of simulation of the kind of small (∼1 nm size) cluster [25] that might exist in our case, too [21], demonstrate that this type of defect cluster also gives rise to a multilevel energy spectrum within the silicon bandgap. An example of such a cluster is shown in figure 7.

The central region of the cluster consists of disordered amorphous-Si like structure generated by ions randomly shifted from their ideal positions. On the opposite sides of the amorphous region, three vacancies and three interstitial ions are placed. A somewhat similar damage structure caused by an HEP was obtained from simulations with TRIM software [32], where it was shown that the vacancy and interstitial enriched regions are spatially separated, and create the dipoles that are important in scattering and recombination of carriers [11, 20]. After the structure generated is allowed to relax, using the DFT molecular dynamics algorithm, down to 0.02 eV Å^{-1} maximal atomic force tolerance, the electron states energy levels are finally calculated. The density of states (DOS) obtained for the relaxed structure pictured in figure 7 is shown in figure 8. It was used a relatively simple DFT procedure sufficient to provide a qualitative picture of the electron states, using the ORCA quantum chemistry program [33] and applied resolution of identity simplification to speed up simulations. The split valence wave-function basis sets SVP (polarized valence double-zeta basis set) and SV/J (accurate Coulomb fitting basis for the SVP basis) and the Becke and Perdew [34] exchange–correlation potential BP86 were used in the DFT calculations. The cluster of 165 Si ions with additional 100 H ions necessary to saturate broken outer Si–Si crystal bonds was chosen for simulations. The ideal structure simulation resulted in a 2.38 Å (Si–Si) bond length and 2.3 eV semiconductor forbidden band gap. We have simulated 20 disordered clusters, expecting to find some common statistical features of the calculated energy levels, however all DOS graphs obtained revealed no significant feature except a random distribution of the energy levels within the forbidden band-gap, as shown in one of examples in figure 8.

It was found that the small relaxed amorphous clusters give rise to states with energy levels closer both to the valence and conduction bands. Therefore, we conclude that the

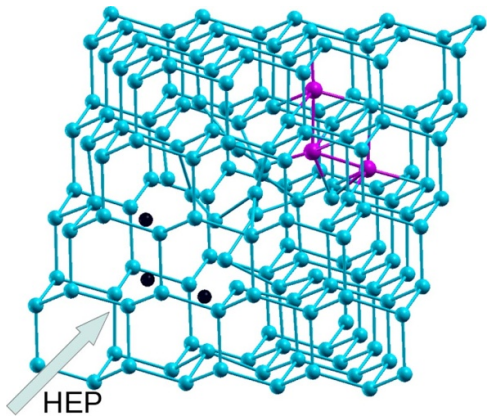

Figure 7. Structure of a small disordered cluster in the crystal damaged by a High Energy Particle (HEP). The arrow shows the incidence direction of HEP. The black spheres are placed at the vacant ideal crystal positions and magenta spheres mark interstitial Si atoms.

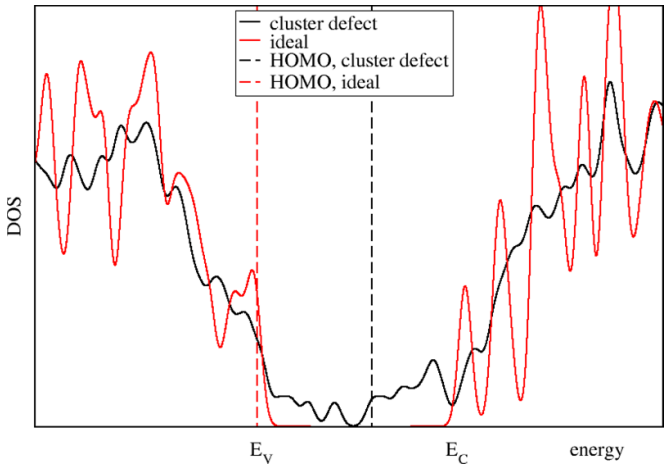

Figure 8. Density of states and the Highest Occupied Molecular Orbital (HOMO) energy levels in fully relaxed crystal structure. The red curve represents the energy states in an ideal Si crystal, while the black one demonstrates the effect of defect clusters in the band gap of the highly irradiated crystals.

additional vacancy and interstitial enriched regions adjacent to an amorphous region prevent its full relaxation, resulting in dense multilevel spectra within the bandgap.

ORCID iDs

Juozas V Vaitkus https://orcid.org/0000-0002-8411-0500
Vaidotas Kažukauskas https://orcid.org/0000-0002-1198-5373
Vilius Vertelis https://orcid.org/0000-0001-5298-5217

References

[1] Adam W *et al* 2017 Characterisation of irradiated thin silicon sensors for the CMS phase II pixel upgrade *Eur. Phys. J.* C **77** 567–80
[2] Pellegrini G *et al* 2016 Recent technological developments on LGAD and iLGAD detectors for tracking and timing applications *Nucl. Instrum. Methods Phys. Res.* A **831** 24–28
[3] Moffat N and Bates R 2021 Simulation of the small pixel effect contributing to a low fill factor for pixellated Low Gain Avalanche Detectors (LGAD) *Nucl. Instrum. Methods Phys. Res.* A **1018** 165746
[4] Cristofoli A, Palestri P, Giordani M P, Cindro V, Dalla Betta G-F and Selmi L 2011 Experimental determination of the impact ionization coefficients in irradiated silicon *IEEE Trans. Nucl. Sci.* **58** 2091–6
[5] Mandić I, Cindro V, Kramberger G and Mikuž M 2009 Measurement of anomalously high charge collection efficiency in n+p strip detectors irradiated by up to 10^{16} n_{eq}/cm^2 *Nucl. Instrum. Methods Phys. Res.* A **603** 263–7
[6] Smith R A 1978 *Semiconductors* (New York: Cambridge University Press)
[7] Macfarlane G G, McLean T P, Quarrington J E and Roberts V 1958 Fine structure in the absorpton-edge specrum of Si *Phys. Rev.* **111** 1245–54
[8] Kalendra V, Gaubas E, Kazukauskas V, Zasinas E and Vaitkus J 2010 Photoconductivity spectra and deep levels in the irradiated p^+–n–n^+ Si detectors *Nucl. Instrum. Methods Phys. Res.* A **612** 555–8
[9] Lucovsky G 1965 On the photoionization of deep impurity centers in semiconductors *Solid State Commun.* **3** 299–302
[10] Vaitkus J V, Mekys A, Rumbauskas V and Storasta J 2016 Neutron irradiation influence on mobility and compensation on dark conductivity in silicon *Lith. J. Phys.* **56** 102–10
[11] Van Zeghbroeck B 2007 *Principles of Semiconductor Devices* (Boulder, CO: University of Colorado)
[12] Vavilov V S and Britsyn K I 1958 Quantum yield of photoionization in silicon *J. Exp. Theor. Phys. (USSR)* **34** 1354
[13] Hodgkinson R J 1963 Impact ionization and quantum efficiency in silicon *Proc. Phys. Soc.* A **82** 1010–9
[14] Christensen O 1976 Quantum efficiency of the internal photoelectric effect in silicon and germanium *J. Appl. Phys.* **47** 689
[15] Antoncik E and Gaur N K S 1978 Theory of the quantum efficiency in silicon and germanium *J. Phys. C: Solid State Phys.* **11** 735–44
[16] McKay K G and McAfee K B 1953 Electron multiplication in silicon and germanium *Phys. Rev.* **91** 1079
[17] Alig R C, Bloom S and Struck C W 1980 Scattering by ionization and phonon emission in semiconductors *Phys. Rev.* B **22** 5565–82
[18] Landsberg P T 1972 On detailed balance between Auger recombination and impact ionization in semiconductors *Proc. Phys. Soc.* A **331** 1584
[19] Reggiani L and Mitin V 1989 Recombination and ionization processes at impurity centres in hot-electron semiconductor transport *Riv. Nuovo Cimento* **12** 1–90
[20] Vaitkus J V, Mekys A and Vaitekonis Š 2021 Electron mobility dependence on neutron irradiation fluence in heavily irradiated silicon *Lith. J. Phys.* **61** 91–96
[21] Huhtinen M 2002 Simulation of non-ionising energy loss and defect formation in silicon *Nucl. Instrum. Methods Phys. Res.* A **491** 194–215
[22] Hastings J L, Estreicher S K and Fedders P A 1997 Vacancy aggregates in silicon *Phys. Rev.* B **56** 10215
[23] Dong J and Drabold D A 1998 Atomistic structure of band-tail states in a-Si *Phys. Rev. Lett.* **80** 1928
[24] Holmström E, Nordlund K and Hakala M 2010 Amorphous defect clusters of pure Si and type inversion in Si detectors *Phys. Rev.* B **82** 104111

[25] Zasinas E and Vaitkus J 2015 Modelling radiation induced vacancy-interstitial clusters *26th RD50 Workshop Book of Abstracts* p 9 (available at: https://indico.cern.ch/event/381195/contributions/905641/attachments/759529/1041866/Vaitkus-RD50-Zasinas_2.pdf)
[26] Drabold D A, Stephan U, Dong J and Nakhmanson S M 1999 The structure of electronic states in amorphous silicon *J. Mol. Graph. Model.* **17** 285–91
[27] Rossum W, Nieuwenhuizen M, Hofstetter E and Schreiber M 1994 Density of states of disordered systems *Phys. Rev.* B **49** 13377
[28] Cartiglia M C N *et al* 2020 LGAD designs for future particle trackers *Nucl. Instrum. Methods Phys. Res.* A **979** 164383
[29] Giedrys T, Grivickas V, Pranevičius L, Ragauskas A and Vaitkus J 1985 Formation of distant recombination centers in Si by ion implantation *Nucl. Instrum. Methods Phys. Res.* B **B6** 427–9
[30] Reznik A, Baranovskii S D, Rubel O, Juska G, Kasap S O, Ohkawa Y, Tanioka K and Rowlands J A 2007 Avalanche multiplication phenomenon in amorphous semiconductors: amorphous selenium versus hydrogenated amorphous silicon *J. Appl. Phys.* **102** 053711
[31] Kramberger G *et al* 2015 Radiation effects in Low Gain Avalanche Detectors after hadron irradiations *J. Instrum.* **10** P07006
[32] Radu R, Pintilie I, Nistor L C, Fretwurst E, Lindstroem G and Makarenko L F 2015 Investigation of point and extended defects in electron irradiated silicon—dependence on the particle energy *J. Appl. Phys.* **117** 164503
[33] Neese F 2012 The ORCA program system *WIREs Comput. Mol. Sci.* **2** 73–78
[34] Becke A D 1988 A multicenter numerical integration scheme for polyatomic molecules *J. Chem. Phys.* **88** 2547